Interaction of an Amphipathic Peptide with Phosphatidycholine/Phosphatidylethanolamine Mixed Membranes

Keisuke Shintou, Minoru Nakano, Tomoari Kamo, Yoshihiro Kuroda, and Tetsurou Handa
Graduate School of Pharmaceutical Sciences, Kyoto University, Kyoto, Japan

ABSTRACT   The effect of 1,2-dioleoyl-*sn*-glycero-3-phosphoethanolamine (DOPE) in mixed membranes with 1-palmitoyl-2-oleoyl-*sn*-glycero-3-phosphocholine (POPC) on interaction with a class A amphipathic peptide, Ac-DWLKAFYDKVAEKLKEAF-NH$_2$ (Ac-18A-NH$_2$), was investigated. The fluorescence lifetime of 2-(9-anthroyloxy)stearic acid and ^{2}H NMR spectra were used to evaluate the penetration of water molecules into the membrane interface and the order of lipid acyl chains, respectively. The results demonstrated that DOPE in the mixed membranes decreased the fluorescence lifetime and increased the acyl-chain order, and that Ac-18A-NH$_2$ affected them more for membranes with higher DOPE fractions. The partition coefficient (K_p) of the peptide to the mixed membranes was increased with the increase in the DOPE mole fractions. From the temperature dependence of the K_p values, the binding of Ac-18A-NH$_2$ to POPC/DOPE mixed membranes was found to be entropy-driven. The formation of an α-helix at the membrane's surface is supposed to induce positive curvature strain, which decreases the headgroup hydration and acyl-chain order of lipids. Thus, the binding of Ac-18A-NH$_2$ to membranes is entropically more favorable at higher DOPE fractions since the peptide's insertion into the membrane can decrease the order parameter and unfavorable headgroup hydration, which explains the enhanced peptide binding.

INTRODUCTION

Biological membranes consist of a variety of lipids, some of which prefer to form nonlamellar structures with a negative curvature and play important roles in membrane dynamics, e.g., membrane fusion and channel opening (1–4). The so-called nonlamellar-forming lipids in bilayers are considered to modify the physicochemical properties of membranes. For example, they increase the lateral pressure in the acyl-chain region due to differences between the membrane's curvature and the spontaneous curvature of the lipid (5–7). The increased lateral pressure is considered to influence the structure of membrane proteins and modulate their functions (5,7–9). In addition, nonlamellar-forming lipids have been shown to increase the activity and binding of certain proteins and peptides that act on membranes. Therefore, detailed observations of the physicochemical properties of membranes containing nonlamellar-forming lipids are required to understand lipid-protein interactions.

Our recent study has demonstrated that the insertion of an amphipathic peptide into the membrane decreases both the penetration of water molecules into the surface and the lateral pressure in the acyl-chain region, and that monoolein (MO), one of the nonlamellar-forming lipids, promotes partitioning of the peptide (10). However, the relationship between the water penetration or lateral pressure and the property of peptide binding has not been clarified from a thermodynamical viewpoint.

In this study, first, we attempted to estimate the lateral pressure and water penetration in 1-palmitoyl-2-oleoyl-*sn*-glycero-3-phosphocholine (POPC)/1,2-dioleoyl-*sn*-glycero-3-phosphoethanolamine (DOPE) mixed membranes. DOPE is a typical nonlamellar-forming lipid possessing a negative spontaneous curvature (11) and is more biologically relevant than MO. DOPE in phospholipid bilayers has been reported to reduce the binding (12) but increase the probability of conductance states of alamethicin (13). Formation of the activated meta II state of rhodopsin from its precursor meta I is promoted in the presence of DOPE (14,15). Next, we examined the effects of an amphipathic α-helical peptide, Ac-DWLKAFYDKVAEKLKEAF-NH$_2$ (Ac-18A-NH$_2$), on the lateral pressure and water penetration. The use of peptides is one of the approaches to obtaining insights into lipid-protein interactions. An amphipathic α-helix has hydrophilic and hydrophobic surfaces and a structure frequently recognized in membrane-associating proteins (16–18). Ac-18A-NH$_2$ forms the amphipathic α-helix and is located at the surface when it associates with the lipid membrane through hydrophobic interactions (19–21). ^{2}H NMR and the fluorescence lifetime of 2-(9-anthroyloxy)stearic acid were determined to evaluate lateral pressure and water penetration, respectively. Finally, a membrane-water partition coefficient of the peptide was determined using large unilamellar vesicles (LUVs) and membrane-peptide interaction was thermodynamically discussed. It is generally accepted that LUVs with a diameter >100 nm have lipid packing density close to planar membranes (22).

EXPERIMENTAL SECTION

Materials

POPC (purity >99%) and 1-palmitoyl-d_{31}-2-oleoyl-*sn*-glycero-3-phosphocholine (POPC-d_{31}, purity >99%) were purchased from Avanti Polar Lipids

(Alabaster, AL). DOPE (purity >99%) was obtained from Sigma Chemical (St. Louis, MO). 2-(9-Anthroyloxy)stearic acid (2-AS) was purchased from Molecular Probes (Eugene, OR). Ac-18A-NH$_2$ was purchased from Takara Bio (Shiga, Japan). Deuterium-depleted water was from Isotec (Tokyo, Japan). These products were used without further purification. All other chemicals were of the highest reagent grade.

Sample preparation

Large unilamellar vesicles (LUVs) of POPC/DOPE mixtures were prepared by the extrusion method. A thin film obtained by evaporating a methanol/chloroform solution of lipids was left under vacuum overnight to remove the residual organic solvent, and was subsequently hydrated with Tris-buffered saline (10 mM Tris-HCl, 150 mM NaCl, pH 7.0). After five rounds of freeze-thawing, the lipid suspension was extruded through a 100-nm pore size polycarbonate filter. The mean particle diameter of each dispersion was ~120 nm, determined from dynamic light scattering measurements (Photal FPAR-1000; Otsuka Electronic, Osaka, Japan).

Multilamellar vesicles (MLVs) of POPC/DOPE mixtures for fluorescence lifetime measurements were prepared as follows. Stock solutions of POPC and DOPE in chloroform were mixed in required proportions. Lipids and a fluorescence probe, 2-AS, were mixed in a methanol/chloroform solution to yield 0.5 mol % 2-AS of total lipids. For the samples containing Ac-18A-NH$_2$, the methanol solution of Ac-18A-NH$_2$ was mixed together to yield 0.5 and 1 mol % of total lipid. After the solvent was evaporated, the sample was dried in a vacuum. Then, Tris-buffered saline was added to the sample at 50 wt % (~700 mM) of the lipid concentration. To achieve homogeneously mixed bilayers, the hydrated sample was vortexed, repeatedly freeze-thawed, and kept at room temperature for 1 week before all measurements. No degradation of lipids was detected by thin-layer chromatography during the sample storage (see Supplementary Material).

For NMR spectroscopy, appropriate phospholipids, POPC-d_{31} (20 mol %) and Ac-18A-NH$_2$, (occasionally) were mixed in a methanol/chloroform mixture. Organic solvents were evaporated and the resulting lipid film was dried under vacuum. The lipid mixtures were hydrated with deuterium-depleted water at 100 mM of the lipid concentration. Finally, three freeze-thaw cycles, with shaking by a vortex mixer, were repeated to achieve better homogeneity.

^{2}H NMR spectroscopy

^{2}H NMR spectra were observed at 25°C on a Varian Unity plus 300 spectrometer (Tokyo, Japan) at 46.044 MHz. MLVs were put into an NMR tube (5 mm o.d.). The quadrupolar echo sequence was used with a 90° pulse of 18.5 μs, interpulse delay of 50 μs, and recycle time of 0.2 s. The spectral width was 80 kHz for 8000 data points. At least 200,000 acquisitions were recorded. Before Fourier transformation, an exponential multiplication was applied to the free induction decay, resulting in a line broadening of 10 Hz. The observed quadrupolar splitting, $\Delta\nu_Q$, is written as $\Delta\nu_Q = 3/4(e^2qQ/h)S_{CD}(n)$, where $e^2qQ/h = 167$ kHz is the quadrupolar coupling constant and $S_{CD}(n)$ is the order parameter.

CD spectral measurements

CD spectra were recorded from 195 to 250 nm with a Jasco J-720 spectropolarimeter at 25°C (Tokyo, Japan). A 0.1-cm path-length cell was used to obtain the peptide spectra at 10 μM in the absence and presence of 2.66 mM LUV. The mean residue ellipticity at 222 nm was used for estimation of the percent helicity of the peptide.

Fluorescence measurements

Front-face illumination was applied to fluorescence lifetime measurements of MLVs (23). The sample was placed between quartz slide glasses. Then,

the sample was set in a cell holder and oriented at an angle of 30° from the incident light to reduce scattered excitation light entering the monochromator, and the foreground emission light was detected.

Fluorescence lifetimes were measured on a Horiba NAES-550 Nanosecond Fluorometer (Kyoto, Japan) with a pulsed hydrogen lamp (full width at half-maximum: ~2 ns) and a thermostated cell holder. The samples labeled with 2-AS were excited through Hoya U360 (Tokyo, Japan) and Toshiba UV-34 filters (Tokyo, Japan) and detected through a CuSO$_4$ solution (250 g/l) and Hoya L42 filters. The fluorescence decay curves were fitted as double-exponentials with convolution of the intensity profile for pulsed excitation light by a Horiba NAES-5X0 lifetime analysis program. The mean lifetime $\langle\tau\rangle$ was defined as

$$\langle\tau\rangle = \sum_{i=1}^{2} \alpha_i\tau_i^2 / \sum_{i=1}^{2} \alpha_i\tau_i, \qquad (1)$$

where α_i and τ_i are the functional amplitude and fluorescence lifetime for the ith component, respectively.

Membrane-water partitioning of peptide

Partitioning of Ac-18A-NH$_2$ between the membrane and water was determined using tryptophan fluorescence by titration with a modification of a previous work (10). Since the end-blocked peptide, Ac-18A-NH$_2$, has greater affinity than the previously used peptide, 18A, titration of Ac-18A-NH$_2$ with LUVs results in the membrane's solubilization. Hence, mixed solutions of LUVs (4 mM) and Ac-18A-NH$_2$ (10 μM) were first prepared and then titrated with Ac-18A-NH$_2$ (10 μM), which reduced the lipid concentration while keeping the peptide concentration constant. Polarizing filters were used to reduce the contribution of scattered light to the emission light (24). The measurement was performed on a Hitachi F-2500 (Tokyo, Japan). Mixed solutions of LUVs and Ac-18A-NH$_2$ in a quartz cell (4 mm in width) were excited using the horizontally polarized incident light at 285 nm, and vertically polarized emission light was detected at 330 nm. The background intensity of LUVs obtained from peptide-free LUV samples was subtracted from the observed fluorescence intensity. Attenuation of fluorescence intensity caused by light scattering of LUVs was corrected by the titration with tryptophan, which does not bind to the membrane. The corrected intensity, I_{corr}, is given by

$$I_{corr} = I_{18A,[L]} \times I_{Trp,0}/I_{Trp,[L]}, \qquad (2)$$

where $I_{18A[L]}$, $I_{Trp[L]}$ are the fluorescence intensities of Ac-18A-NH$_2$ and tryptophan at each lipid concentration, respectively, and $I_{Trp,0}$ is the fluorescence intensity of tryptophan in the absence of LUVs.

The partition coefficient is determined according to Nakagaki et al. (25). The theory is as follows: The peptide tryptophan fluorescence intensity in the presence of LUV, I, is expressed by

$$I = f_f c_f + f_b c_b, \qquad (3)$$

where c_f, c_b are the lipid-free and lipid-bound peptide concentrations, respectively, and f_f, f_b are the molar fluorescence constants of the lipid-free and lipid-bound peptides, respectively. The fluorescence intensity in the absence of LUV, I_0, is given by

$$I_0 = f_f c_t, \qquad (4)$$

$$c_t = c_f + c_b, \qquad (5)$$

where c_t is the total peptide concentration. From Eqs. 3–5, the increase of fluorescence intensity after mixing with LUV, ΔI, is

$$\Delta I = I - I_0 = c_b(f_b - f_f). \qquad (6)$$

The mole-ratio partition coefficient, K_p, is expressed by

$$K_p = \frac{c_b/[L]}{c_f/[W]}, \tag{7}$$

where $[L]$ is the lipid concentration at outer leaflets of vesicles and $[W] = 55.5$ M is the water concentration. The outer/inner ratio of phospholipids was determined by a ^{31}P NMR method with a bilayer-impermeable paramagnetic ion (26). From Eqs. 5–7,

$$c_t = \frac{\Delta I}{[L](f_b - f_f)}\left([L] + \frac{[W]}{K_p}\right), \tag{8}$$

which gives

$$\frac{[L]}{\Delta I} = \frac{1}{c_t(f_b - f_f)}\left([L] + \frac{[W]}{K_p}\right). \tag{9}$$

A plot of $[L]/\Delta I$ against $[L]$ according to Eq. 9 yields a straight line, and K_p can be determined from the slope and intercept.

Ac-18A-NH$_2$ binding assay by ultracentrifugation

A mixture (500 μL) of POPC LUV (4 mM) and Ac-18A-NH$_2$ (30 μM) was incubated for 1 h to equilibrate the free and bound peptides at 25 and 35°C. After the addition of 5% sucrose to adjust the density, each mixture was ultracentrifuged (100,000 g) to separate the bound (the top fraction) from free peptide (the bottom fraction, 200 μL). The centrifugation period of 2 h was selected to give stationary values for bound peptide. The bottom fraction was mixed with 100 μL of 10% nonionic surfactant, hepta-ethylene-glycol-mono-dodecyl ether, and left overnight at 4°C to solubilize the small amounts of remaining lipid (27). The free peptide concentration was determined by measuring the Trp fluorescence at 330 nm (excitation at 285 nm). The bound peptide concentration was calculated from the free and total peptide concentrations.

RESULTS

In this study, we used POPC/DOPE mixtures with DOPE mole fractions of 0, 0.3, and 0.5. The formation of non-lamellar phases was not observed for these mixtures at the temperatures at which the experiments were performed (20–35°C).

Penetration of water molecules into POPC/DOPE mixed membranes

The fluorescence lifetimes of fluorophores are sensitive to changes in temperature and their surrounding polarity and can be a measure of penetration of water (28–30). The fluorescence lifetime of 2-AS was measured to determine the degree to which water molecules penetrate the surface of the POPC/DOPE mixed membranes. Since the fluorophore of 2-AS is located in the hydrophobic region near the membrane surface, a decrease in the fluorescence lifetime represents an increased hydration near carbonyl groups of lipids. Recent study with NMR and neutron diffraction on POPC bilayers revealed that water molecules penetrated and interacted with sites of the interfacial region of bilayers, including choline, phosphate, glycerol, and carbonyl groups (31). The mean lifetime $\langle \tau \rangle$ of 2-AS in the membranes at 25 and 30°C is

shown in Fig. 1, A and B, respectively, as a function of the molar ratio of Ac-18A-NH$_2$. The $\langle \tau \rangle$ values decreased with the DOPE fractions. This result represents that the non-lamellar-forming lipid with small headgroup relative to the hydrophobic volume decreases the 2-AS fluorescence lifetime within the interface region of bilayers (10).

The addition of Ac-18A-NH$_2$ increased $\langle \tau \rangle$ values in a concentration-dependent manner. It should be noted that all the peptides can be assumed to bind to the membrane under the experimental conditions ($\sim$700 mM of lipid). In addition, the increment of $\langle \tau \rangle$ was more pronounced at higher DOPE fractions, suggesting that the peptide is more effective at reducing the penetration of water at higher DOPE fractions. Similar results were obtained at 25 and 30°C, while $\langle \tau \rangle$ was reduced at higher temperature due to an increase in the
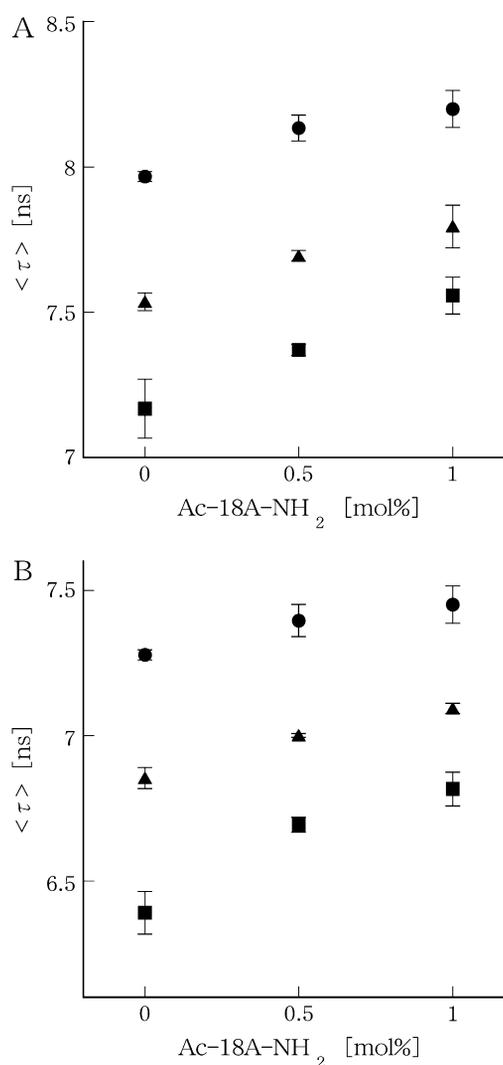

FIGURE 1 The mean fluorescence lifetime $\langle \tau \rangle$ of 2-AS in POPC/DOPE mixed membranes with DOPE mole fractions of 0 (*solid circles*), 0.3 (*solid triangles*), and 0.5 (*solid squares*) as a function of the molar ratio of Ac-18A-NH$_2$ to total lipid at 25°C (*A*) and 30°C (*B*). Each point represents the mean ± SD of three samples.

collision frequency of the fluorophores with water molecules.

Order parameter of POPC/DOPE membranes

^{2}H NMR experiments were performed with lipid mixtures (MLVs) containing POPC-d_{31} to investigate the effect of DOPE and Ac-18A-NH$_2$ in the acyl-chain region of the membranes. ^{2}H NMR quadrupolar splitting is proportional to the local orientational order parameter, $S_{CD}(n)$, defined by $S_{CD}(n) = \langle 3\cos^2\theta_n - 1 \rangle/2$, where θ_n is the angle between the C-D bond for the nth carbon position and the symmetry axis of the rapid motions of the acyl chain. The angular brackets represent an average over molecular conformation and orientation on the NMR timescale.

The order parameter for each carbon site of the lipid acyl chain is given in Fig. 2 for POPC/DOPE membranes at 25°C in the absence and presence of Ac-18A-NH$_2$, where all the peptides added are bound with the membranes. In the absence of Ac-18A-NH$_2$, the order parameter increased with the DOPE fractions. Since order parameters are inversely related to the molecular area of lipids (32), this result represents that DOPE induces tighter packing in the acyl chains of POPC. The addition of Ac-18A-NH$_2$ decreased the order parameter as shown in Fig. 2. The data are obtained from single experiment and thus their uncertainties and significances are not discernable. In addition, freeze-thaw cycles in the sample preparation possibly produce small vesicles that influence the data (33). However, the results could represent that insertion of the peptides at the membrane interface induces positive curvature strain, which decreases the acyl-chain order. This is consistent with our previous results in POPC/MO mixtures, where the increased lateral pressure by MO, which
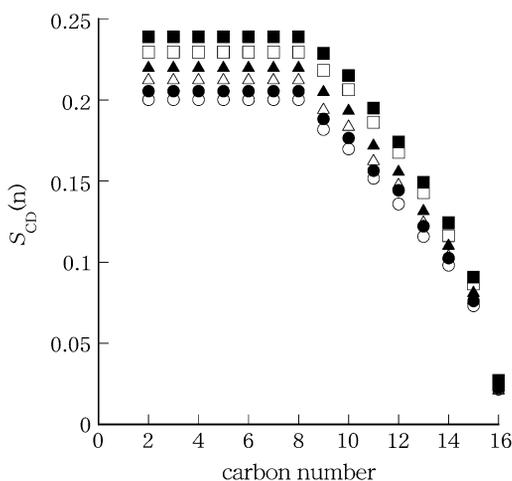
was estimated by excimer formation of dipyrenyl-PC, was reduced by Ac-18A-NH$_2$ (10).

Partitioning of the amphipathic peptide to the POPC/DOPE membranes

The membrane-water partition coefficient (K_p) of Ac-18A-NH$_2$ was calculated using POPC/DOPE LUVs to evaluate the effect of DOPE on the binding. As shown in Fig. 3, the plot of $[L]/\Delta I$ as a function of $[L]$ exhibited a good linear relationship, from which K_p was determined. The K_p value of Ac-18A-NH$_2$ for the pure POPC membrane (1.32×10^5) was sevenfold higher than that of the end-unblocked peptide, 18A (10). The van't Hoff plot for each POPC/DOPE membrane showed a linear relationship over the temperature range examined (Fig. 4). A negative slope means that the peptide binding is an endothermic process. The thermodynamic parameters determined are listed in Table 1. The standard Gibbs free energy change accompanied by the peptide binding is more negative at higher DOPE fractions, representing that the binding is energetically more favorable. The peptide binding process was found to be driven by entropy but opposed by enthalpy. In addition, ΔH^0 and ΔS^0 increased with the DOPE fractions. Thus, it can be concluded that DOPE promotes the peptide binding by making its process entropically more favorable.

α-Helical content

From the CD spectra, the α-helical content of Ac-18A-NH$_2$ (10 μM) in the presence of 2.66 mM POPC/DOPE LUVs was determined as 55.2, 64.7, and 68.5% for 0, 30, and 50% DOPE, respectively. Using these values with the α-helical
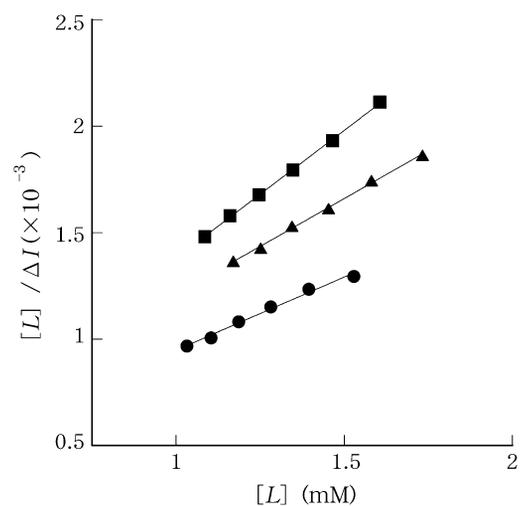

FIGURE 2 Order parameter for each carbon site of POPC palmitoyl chains in POPC/DOPE mixed membranes with DOPE mole fractions of 0 (*circles*), 0.3 (*triangles*), and 0.5 (*squares*) in the absence (*solid symbols*) and presence (*open symbols*) of 1 mol % Ac-18A-NH$_2$ at 25°C.

FIGURE 3 Typical titration results of the partitioning of Ac-18A-NH$_2$ to POPC/DOPE mixed membranes with DOPE mole fractions of 0 (*solid circles*), 0.3 (*solid triangles*), and 0.5 (*solid squares*) at 25°C. $[L]/\Delta I$ was plotted against $[L]$, and K_p was determined from the slope and intercept.
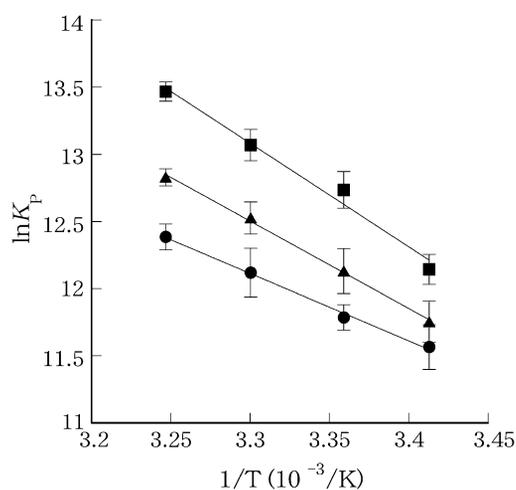
FIGURE 4 van't Hoff plot for Ac-18A-NH$_2$ binding to POPC/DOPE LUVs with DOPE mole fractions of 0 (*solid circle*), 0.3 (*solid triangle*), and 0.5 (*solid square*). Each point represents the mean ± SD of three samples.

content in buffer (21.5%) and K_p for each membrane (Table 1), percent helicity of the peptide on membranes was determined, and is summarized in Table 2. DOPE was found to slightly increase the helicity of the peptide on the membranes but significant differences were not found.

Determination of the peptide binding by ultracentrifugation

To confirm that the peptide binding is entropy-driven, the binding amount was directly determined by ultracentrifugation. The free peptide concentration in the mixture of Ac-18A-NH$_2$ (30 μM) and POPC LUV (4 mM) was 8.5 and 5.7 μM at 25 and 35°C, respectively, representing an enhanced binding at higher temperature. From these binding data, K_p at 25 and 35°C was calculated at 0.89×10^5 and 1.50×10^5, respectively, which was smaller but close to the value obtained by titration (1.32×10^5 and 2.40×10^5, respectively).

DISCUSSION

The results presented here show that the binding of an amphipathic α-helical model peptide, Ac-18A-NH$_2$, to phospholipid membranes is promoted by the presence of a nonlamellar-forming lipid, DOPE. This result is consistent with a pre-

TABLE 1 Thermodynamic parameters for partitioning of Ac-18A-NH$_2$ to POPC/DOPE LUVs at 25°C

Mole fraction of DOPE	$K_p \times 10^{-5}$	ΔG^0 (kcal/mol)	ΔH^0 (kcal/mol)	$T\Delta S^0$ (kcal/mol)
0	1.32 ± 0.13	−6.98 ± 0.06	10.00 ± 0.43	16.98 ± 0.42
0.3	1.87 ± 0.32	−7.19 ± 0.10	12.75 ± 0.28	19.94 ± 0.28
0.5	3.41 ± 0.45	−7.54 ± 0.08	15.31 ± 1.42	22.81 ± 1.46

Values are the means ± SD from three experiments.

TABLE 2 α-Helix content of Ac-18A-NH$_2$ on POPC/DOPE membranes at 25°C

Mole fraction of DOPE	% Helicity on membranes	Δ% Helicity*	ΔH^0_{helix} [†] (kcal/mol)	$T\Delta S^0_{helix}$ [‡] (kcal/mol)
0	69.4 ± 5.0	47.9 ± 5.0	−6.0 ± 0.6	−4.9 ± 0.5
0.3	75.4 ± 7.3	53.9 ± 7.3	−6.8 ± 0.9	−5.5 ± 0.7
0.5	76.2 ± 1.7	54.7 ± 1.7	−6.9 ± 0.2	−5.6 ± 0.2

Values are the means ± SD from three experiments.
*Δ% Helicity = %Helicity on membranes − %Helicity in buffer (21.5%).
[†]$\Delta H^0_{helix,residue}$ = −0.7 (kcal/mol) per residue (39).
[‡]$\Delta S^0_{helix,residue}$ = −1.9 (cal/mol K) per residue (39).

vious report, where the binding of 18A to the POPC/MO mixed membrane increased with the fractions of the nonlamellar-forming lipid (10).

DOPE in planar bilayers was found to increase acyl-chain packing (Fig. 2) but concomitantly decrease the lifetime of 2-AS at the interface (Fig. 1). Ho et al. (34) have observed similar effects of phosphatidylethanolamine, which decreases interchain hydration and increases headgroup hydration in phospholipid bilayers. They used 1-palmitoyl-2-[[2-[4-(6-phenyl-1,3,5-hexatrienyl)phenyl] ethyl]carbonyl]-3-*sn*-glycero-3-phosphocholine (DPH-PC) and *N*-(5-dimethylaminonaphthalene-1-sulfonyl) dipalmitoylphosphatidyl-ethanolamine and revealed that interchain hydration estimated from the fluorescence lifetime of DPH-PC correlated with acyl-chain order that was independent of lipid composition, while acyl-chain order (or interchain hydration) is uncoupled with headgroup hydration (34). The increase in headgroup hydration is, however, considered to be energetically unfavorable for DOPE, since it has a smaller headgroup and thus can bind a lesser amount of water molecules than POPC. This packing constraint, as well as acyl-chain order, can be released by lamellar-nonlamellar phase transition (10,35), by which the cross-sectional molecular area at the polar group-water interface is decreased and the area at the terminal methyl ends of the acyl chains is increased (36). Binding of molecules that provide positive curvature to the membranes is another way to get rid of the constraints, and Ac-18A-NH$_2$ is the case.

It has been reported that the interaction of Ac-18A-NH$_2$ with vesicles is enthalpically and entropically favored, although the magnitude of ΔH^0 and ΔS^0 depends on the vesicle size (37). In this study, we double-checked by titration and ultracentrifugation that the peptide binding to POPC LUV (~120 nm) is driven by entropy. From the thermodynamic point of view, it is instructive to consider the molecular sources of the measured ΔH^0 and ΔS^0. The binding reaction of Ac-18A-NH$_2$ was shown to be an entropy-driven process. This means that the binding of Ac-18A-NH$_2$ is endothermic and the lipid-peptide complex has a higher internal energy than the individual lipid and peptide starting materials. ΔH^0 and ΔS^0 include 1), the conformational changes in the peptide molecules; 2), the peptide transition effects such as the displacement of the water molecules from both peptide and membrane surfaces, and the protonation/deprotonation reaction of

basic and acid groups in the peptide (38); and 3), the perturbation of the lipid membrane structure as a result of the binding.

Conformational changes in the peptide molecules

Binding of the peptide to membranes is often accompanied by a random coil-α helix transition. The main reason for a membrane-induced helix is that the helix-forming tendency of a peptide is considerably higher in the hydrophobic environment of the membrane than in water. The formation of a helix is driven by enthalpy ($\Delta H^0_{\text{helix,residue}} = -0.7$ kcal/mol per residue), but opposed by entropy ($\Delta S^0_{\text{helix,residue}} = -1.9$ cal/mol K per residue) (39). Exothermic components of enthalpy, $\Delta H^0_{\text{helix}}$, due to an increase in helicity, have ranged from -6.0 kcal/mol (POPC) to -6.9 kcal/mol (POPC/DOPE (5/5)). Similarly, an increase in helicity leads to a decrease in entropy with predicted range of $T\Delta S^0_{\text{helix}}$ from -4.9 kcal/mol (POPC) to -5.6 kcal/mol (POPC/DOPE (5/5)). Since both ΔH^0 and ΔS^0 are positive (Table 1), other effects that drive the binding must be taken into account.

Peptide transition effects

In zwitterionic POPC and DOPE model membranes, van der Waals interaction, and the formation of hydrogen bonds between the peptide and lipids are exothermic in nature. However, the peptide binding could be in part counteracted by the endothermic reaction associated with the release of ordered water molecules from both the peptide and membrane surfaces, which involves the breakage of hydrogen and ionic bonds. The fluorescence lifetime of 2-AS is decreased at higher DOPE fractions, which is more effectively inhibited by the peptide binding. Therefore, enthalpy change of the peptide insertion increases with the DOPE fractions since more energy is required to break hydrogen bonds between water molecules and membranes. On the other hand, the release of the ordered water molecules is a process accompanied by an increase in the entropy of the system. This effect induced by the amphipathic peptide binding is pronounced for the membranes with a higher degree of hydration. The peptide binding is thus considered to be an entropy-driven process and the entropic contribution to this system is larger at higher DOPE fractions.

Perturbation of the lipid membrane structure

An important surface phenomenon that would amount to a positive component of the enthalpy may originate from the perturbation of the lipid membrane structure or from the peptide-induced increase of the membrane area on the peptide's insertion. Increasing the membrane surface area against surface tension to allow for peptide binding amounts to an increase in enthalpy, $\Delta H^0_{\text{bilayer}}$ (40). However, membranes with higher DOPE fractions could require less of an increase in the area because the smaller headgroup of DOPE gives

more space to accommodate peptide adsorption (41), which would have resulted in the decreased $\Delta H^0_{\text{bilayer}}$ with DOPE. Rather, the replacement of lipid-lipid molecular interactions with lipid-peptide interactions by the peptide insertion could be predominant for the enthalpy change. Since Ac-18A-NH$_2$ may not pack as well with the surrounding lipid molecules, the replacement will lead to high endothermic enthalpy, especially, in more well-ordered membrane systems.

The increase in the area of the membrane upon binding of the peptide leads to a proportionally large entropy increase ($\Delta S^0_{\text{bilayer}}$) due to the disordering of the acyl hydrocarbon chains (40). As shown in Fig. 2, the addition of Ac-18A-NH$_2$ decreases the acyl chain's order parameter for all carbon sites, suggesting that Ac-18A-NH$_2$ decreased the lateral pressure in the acyl-chain region of the membranes. Thus, the peptide-induced increase in area of the membranes, which subsequently causes the increase in the disorder of the membrane lipids, could be an additional driving force for the peptide binding to the POPC/DOPE mixed membranes as well as the peptide transition effects discussed above.

SUPPLEMENTARY MATERIAL

To view all of the supplemental files associated with this article, visit www.biophysj.org.

REFERENCES

1. van Dalen, A., and B. de Kruijff. 2004. The role of lipids in membrane insertion and translocation of bacterial proteins. *Biochim. Biophys. Acta.* 1694:97–109.

2. van Dalen, A., S. Hegger, J. A. Killian, and B. de Kruijff. 2002. Influence of lipids on membrane assembly and stability of the potassium channel KcsA. *FEBS Lett.* 525:33–38.

3. van Klompenburg, W., M. Paetzel, J. M. de Jong, R. E. Dalbey, R. A. Demel, G. von Heijne, and B. de Kruijff. 1998. Phosphatidylethanolamine mediates insertion of the catalytic domain of leader peptidase in membranes. *FEBS Lett.* 431:75–79.

4. Yang, L., L. Ding, and H. W. Huang. 2003. New phases of phospholipids and implications to the membrane fusion problem. *Biochemistry.* 42:6631–6635.

5. Bezrukov, S. M. 2000. Functional consequences of lipid packing stress. *Curr. Opin. Colloid Interface Sci.* 5:237–243.

6. Lafleur, M., M. Bloom, E. F. Eikenberry, S. M. Gruner, Y. Han, and P. R. Cullis. 1996. Correlation between lipid plane curvature and lipid chain order. *Biophys. J.* 70:2747–2757.

7. van den Brink-van der Laan, E., J. A. Killian, and B. de Kruijff. 2004. Nonbilayer lipids affect peripheral and integral membrane proteins via changes in the lateral pressure profile. *Biochim. Biophys. Acta.* 1666: 275–288.

8. de Kruijff, B. 1987. Polymorphic regulation of membrane lipid composition. *Nature.* 329:587–588.

9. Lee, A. G. 2004. How lipids affect the activities of integral membrane proteins. *Biochim. Biophys. Acta.* 1666:62–87.

10. Kamo, T., M. Nakano, Y. Kuroda, and T. Handa. 2006. Effects of an amphipathic α-helical peptide on lateral pressure and water penetration in phosphatidylcholine and monoolein mixed membranes. *J. Phys. Chem. B*. 110:24987–24992.

11. Israelachvili, J. N., S. Marcelja, and R. G. Horn. 1980. Physical principles of membrane organization. *Q. Rev. Biophys.* 13:121–200.

12. Lewis, J. R., and D. S. Cafiso. 1999. Correlation between the free energy of a channel-forming voltage-gated peptide and the spontaneous curvature of bilayer lipids. *Biochemistry*. 38:5932–5938.

13. Keller, S. L., S. M. Bezrukov, S. M. Gruner, M. W. Tate, I. Vodyanoy, and V. A. Parsegian. 1993. Probability of alamethicin conductance states varies with nonlamellar tendency of bilayer phospholipids. *Biophys. J.* 65:23–27.

14. Botelho, A. V., N. J. Gibson, R. L. Thurmond, Y. Wang, and M. F. Brown. 2002. Conformational energetics of rhodopsin modulated by nonlamellar-forming lipids. *Biochemistry*. 41:6354–6368.

15. Brown, M. F. 1994. Modulation of rhodopsin function by properties of the membrane bilayer. *Chem. Phys. Lipids*. 73:159–180.

16. Segrest, J. P., R. L. Jackson, J. D. Morrisett, and A. M. Gotto, Jr. 1974. A molecular theory of lipid-protein interactions in the plasma lipoproteins. *FEBS Lett.* 38:247–258.

17. Segrest, J. P., M. K. Jones, H. De Loof, C. G. Brouillette, Y. V. Venkatachalapathi, and G. M. Anantharamaiah. 1992. The amphipathic helix in the exchangeable apolipoproteins: a review of secondary structure and function. *J. Lipid Res.* 33:141–166.

18. Kalmar, G. B., R. J. Kay, A. Lachance, R. Aebersold, and R. B. Cornell. 1990. Cloning and expression of rat liver CTP: phosphocholine cytidylyltransferase: an amphipathic protein that controls phosphatidylcholine synthesis. *Proc. Natl. Acad. Sci. USA*. 87:6029–6033.

19. Hristova, K., W. C. Wimley, V. K. Mishra, G. M. Anantharamaiah, J. P. Segrest, and S. H. White. 1999. An amphipathic α-helix at a membrane interface: a structural study using a novel x-ray diffraction method. *J. Mol. Biol.* 290:99–117.

20. Clayton, A. H., and W. H. Sawyer. 1999. Tryptophan rotamer distributions in amphipathic peptides at a lipid surface. *Biophys. J.* 76:3235–3242.

21. Clayton, A. H., and W. H. Sawyer. 1999. The structure and orientation of class-A amphipathic peptides on a phospholipid bilayer surface. *Eur. Biophys. J.* 28:133–141.

22. Wieprecht, T., M. Beyermann, and J. Seelig. 2002. Thermodynamics of the coil-α-helix transition of amphipathic peptides in a membrane environment: the role of vesicle curvature. *Biophys. Chem.* 96:191–201.

23. Lakowicz, J. R. 1999. Principles of Fluorescence Spectroscopy, 2nd Ed. Kluwer Academic/Plenum Publishers, New York.

24. Ladokhin, A. S., S. Jayasinghe, and S. H. White. 2000. How to measure and analyze tryptophan fluorescence in membranes properly, and why bother? *Anal. Biochem.* 285:235–245.

25. Nakagaki, M., H. Komatsu, and T. Handa. 1986. Estimation of critical micelle concentrations of lysolecithins with fluorescent probes. *Chem. Pharm. Bull.* (*Tokyo*). 34:4479–4485.

26. Saito, H., K. Nishiwaki, T. Handa, S. Ito, and K. Miyajima. 1995. Comparative study of fluorescence anisotropy in surface monolayers of emulsions and bilayers of vesicles. *Langmuir*. 11:3742–3747.

27. Saito, H., Y. Miyako, T. Handa, and K. Miyajima. 1997. Effect of cholesterol on apolipoprotein A-I binding to lipid bilayers and emulsions. *J. Lipid Res.* 38:287–294.

28. Straume, M., and B. J. Litman. 1987. Influence of cholesterol on equilibrium and dynamic bilayer structure of unsaturated acyl chain phosphatidylcholine vesicles as determined from higher order analysis of fluorescence anisotropy decay. *Biochemistry*. 26:5121–5126.

29. Straume, M., and B. J. Litman. 1987. Equilibrium and dynamic structure of large, unilamellar, unsaturated acyl chain phosphatidylcholine vesicles. Higher order analysis of 1,6-diphenyl-1,3,5-hexatriene and 1-[4-(trimethylammonio)phenyl]- 6-phenyl-1,3,5-hexatriene anisotropy decay. *Biochemistry*. 26:5113–5120.

30. Fiorini, R. M., M. Valentino, M. Glaser, E. Gratton, and G. Curatola. 1988. Fluorescence lifetime distributions of 1,6-diphenyl-1,3,5-hexatriene reveal the effect of cholesterol on the microheterogeneity of erythrocyte membrane. *Biochim. Biophys. Acta*. 939:485–492.

31. Gawrisch, K., H. C. Gaede, M. Mihailescu, and S. H. White. 2007. Hydration of POPC bilayers studied by H-1-PFG-MAS-NOESY and neutron diffraction. *Eur. Biophys. J. Biophys.* 36:281–291.

32. Petrache, H. I., S. W. Dodd, and M. F. Brown. 2000. Area per lipid and acyl length distributions in fluid phosphatidylcholines determined by H-2 NMR spectroscopy. *Biophys. J.* 79:3172–3192.

33. Traikia, M., D. E. Warschawski, M. Recouvreur, J. Cartaud, and P. F. Devaux. 2000. Formation of unilamellar vesicles by repetitive freeze-thaw cycles: characterization by electron microscopy and P-31-nuclear magnetic resonance. *Eur. Biophys. J. Biophys.* 29:184–195.

34. HO, C., S. J. Slater, and C. D. Stubbs. 1995. Hydration and order in lipid bilayers. *Biochemistry*. 34:6188–6195.

35. Nakano, M., T. Karno, A. Sugita, and T. Handa. 2005. Detection of bilayer packing stress and its release in lamellar-cubic phase transition by time-resolved fluorescence anisotropy. *J. Phys. Chem. B*. 109:4754–4760.

36. Gawrisch, K., V. A. Parsegian, D. A. Hajduk, M. W. Tate, S. M. Gruner, N. L. Fuller, and R. P. Rand. 1992. Energetics of a hexagonal lamellar hexagonal-phase transition sequence in dioleoylphosphatidylethanolamine membranes. *Biochemistry*. 31:2856–2864.

37. Gazzara, J. A., M. C. Phillips, S. Lund-Katz, M. N. Palgunachari, J. P. Segrest, G. M. Anantharamaiah, W. V. Rodrigueza, and J. W. Snow. 1997. Effect of vesicle size on their interaction with class A amphipathic helical peptides. *J. Lipid Res.* 38:2147–2154.

38. Beschiaschvili, G., and J. Seelig. 1992. Peptide binding to lipid bilayers. Nonclassical hydrophobic effect and membrane-induced pK shifts. *Biochemistry*. 31:10044–10053.

39. Wieprecht, T., O. Apostolov, M. Beyermann, and J. Seelig. 1999. Thermodynamics of the α-helix-coil transition of amphipathic peptides in a membrane environment: implications for the peptide-membrane binding equilibrium. *J. Mol. Biol.* 294:785–794.

40. Abraham, T., R. N. Lewis, R. S. Hodges, and R. N. McElhaney. 2005. Isothermal titration calorimetry studies of the binding of a rationally designed analogue of the antimicrobial peptide gramicidin s to phospholipid bilayer membranes. *Biochemistry*. 44:2103–2112.

41. Lee, M. T., W. C. Hung, F. Y. Chen, and H. W. Huang. 2005. Many-body effect of antimicrobial peptides: on the correlation between lipid's spontaneous curvature and pore formation. *Biophys. J.* 89:4006–4016.